Paper ID ICLASS06-248
MORPHOLOGY AND FLUCTUATIONS OF A LIQUID JET IN HIGH-DENSITY AIR CROSSFLOW

A. Bellofiore [1], R. Ragucci [2], P. Di Martino [3] and A. Cavaliere [1]

[1]Dept. of Chemical Engineering, University Federico II of Naples, ITALY, abellofi@unina.it, antcaval@unina.it
[2]Istituto di Ricerca sulla Combusttione, CNR, Naples, ITALY, ragucci@irc.cnr.it
[3]Avio Group, Pomigliano d'Arco, Naples, ITALY, pasquale.dimartino@aviogroup.com

ABSTRACT This paper presents a study on morphology and instability of a liquid injected in crossflow. Image statistical analysis procedures are described and applied to a database of about 300 experimental conditions obtained by injecting jet-A1 and water in a high-density crossflow at different air pressures and temperatures. For each condition a sample of 1000 shadowgraphic images is available. The study is conducted on both native and binary images. The mean and the standard deviation of the intensity of light extinction are evaluated for each pixel of the image. On the basis of the average binary images the definition of spray centerline is introduced as a suitable curvilinear coordinate. The centerline allows for defining, also for jets in crossflow, a spray angle, which results to depend on liquid Weber number and orifice diameter. The standard deviation of native images points out the existence of a small stable region near the injection point. The standard deviation of binary images, accounting for jet whipping, is used to evaluate an intermittency index, which decreases as the momentum ratio increases.

Keywords: Crossflow Atomization, Image Statistical Analysis, Spray Centerline, Spray Angle, Spray Intermittency.

1. INTRODUCTION

Liquid jets in air crossflow are relevant in many applications of momentum, heat and mass transfer when the access in the gas flow is only through external walls [1] and when high level of momentum is needed in order to mix more uniformly a liquid fuel in air stream [2]. One of the most interesting applications of these configurations is in Lean Premixed Prevaporized gas turbine [3]. In this case the optimization of fuel premixing requires the achievement of an as much as possible uniform fuel distribution in the air stream, and hence of the combustion temperature distribution, not only to minimize pollutant formation but also to reduce the onset of combustion instabilities problems that affect these devices. The use of one or more plain nozzles that inject the fuel, with a suitable geometry, in the air stream benefits of the more stable characteristics of this atomization in respect of swirled pressure nozzle.

The characteristics of the liquid jets fragmentation have been studied by many authors, who focused mainly on the topology of the jet bending [2,4,5] and on the breakup distance from the nozzle [1], at which the liquid primary atomization is ended [6]. The authors of the present paper have presented several studies on this subject [7-11]. One of the main achievements of these studies is represented by the Eq. (1) [12,13], which represents the curvilinear upstream edge of the spray, which is commonly assumed as representative of the trajectory of the liquid jet.

$$\frac{z}{z_{jb}} = \left(\frac{x}{x_{jb}} \right)^{0.367} \tag{1}$$

Equation (1) implies that the coordinates of the jet trajectory, along the geometrical axis of the liquid jet nozzle (z) and the gas stream (x), when they are scaled by the parameters x_{jb} and z_{jb}, follow the same power law for whatever external parameter conditions, which include the liquid-to-air momentum ratio $q = \rho_L V_L^2 / \rho_G V_G^2$ up to values of 300, air density up to 20 Kg/m^3, liquid and gas velocity up to 55 m/s, nozzle diameters between 300 μm and 500 μm and surface tensions between values of water at 300 K (0.072 N/m) and Jet A-1 at 600 K (0.022 N/m). The two parameters are the measured coordinates of the jet breakdown, i.e. of the point along the jet trajectory where the profiles of the jet became essentially unsteady and after which they change sample-by-sample. A simple statistical study of the jet unsteadiness allows the determination of this point with a simple, repeatable and quantitative automatic procedure [12]. The features of this procedure remove all the arbitrariness due to the subjectivity in the individuation of the jet trajectory and mainly of breakup point that characterizes previous studies in this field. The jet breakdown refers to the level of coherence of the momentum, analogously to what has been defined for gas swirled jet behavior. It is not straightly correlated to the breakup point, where the liquid undergoes significant rupture, because the liquid may keeps its momentum also in presence of fragmentation in blobs or large droplets, which do not increase the specific liquid-air interface significantly.

The jet breakdown coordinates were found to be a function of the nozzle diameter D, of the aerodynamic Weber number $We_{aero} = \rho_G V_L^2 D / \sigma$ and of the momentum ratio, q, according to Eqs. (2) and (3) in the same parameter ranges where Eq. (1) has been validated. A weaker dependence on the air viscosity was also assessed.

$$\frac{x_{jb}}{D} = 4.17\ q^{-0.095}\ We_{aero}^{0.382} \left(\frac{\mu}{\mu_{air,\ 300K}} \right)^{0.046} \tag{2}$$

$$\frac{z_{jb}}{D} = 3.85\ q^{0.387}\ We_{aero}^{0.126} \left(\frac{\mu}{\mu_{air,\ 300K}} \right)^{0.202} \tag{3}$$

It is noteworthy that the jet breakdown position defines precisely the dominion, in which Eqs. (1-3) describe the liquid profile, and that it also depends on the liquid surface tension differently from what have been reported in previous literature works [1,14]. This main difference is due to the fact that Eqs. (1-3) have been validated in a wider dominion in respect to the other works and, in particular, in a higher liquid velocity range. This in turn makes the Weber number influence on Eq. (2) appreciable through its quadratic dependence on liquid velocity. This also reflects the fact that the liquid jet undergoes significant atomization due to the liquid dynamic pressure prevalence on the capillary pressure and an enhanced reduction of the column diameter has to be expected.

This paper presents a study on morphology and stability of a liquid injected in crossflow. Image statistical analysis procedures were developed and applied to a database of about 250 experimental conditions obtained by injecting jet-A1 and water in a high-density crossflow at different air pressures and temperatures. The followed methodology is extensively described in this paper, along with some interesting results about the definitions of spray centerline and spray angle. The concept of instability and intermittency are discussed, and a measure of the overall level of intermittency of the spray is presented.

2. EXPERIMENTALS

The experimental apparatus used in the preparation of this paper was aimed to reproduce the working conditions occurring in the premixing duct of an LPP gas turbine. An optically accessible channel with 25x25 mm^2 cross-section is swept by the compressed and pre-heated airflow. One of the sidewalls houses a plain orifice injector. Details of the experimental facility are available in Ref. [12].

The shadowgraphic scheme reported in Fig. 1 was adopted to collect images of the spray. The devices used for this purpose are a Xenon flash lamp with pulse length of 15 µs, a Pulnix TM-6710 digital camera, set up to acquire 8-bit 640x200 pixel frames at 240 Hz, and a BNC delay generator for time base generation and synchronization. For each test condition a set of 1000 frames was collected.

The complete database referred to in this paper includes measurements on jet-A1 and water. A concise synopsis is reposted in table 1, along with the abbreviations (in red) used in the following to name the several test cases. The values of surface tension of jet-A1 and water at 600 K air temperature are assessed as described in [13].

Table 1. Synoptic scheme of the test cases.

		10 bar (10)	16 bar (16)	20 bar (20)	
		300 K (F)	600 K (C)	300 K (F)	600 K (C)
water (W)	nozzle 0.3 (3)	W3F10			W3C20
	nozzle 0.5 (5)	W5F10		W5F20	W5C20
kerosene (K)	nozzle 0.3 (3)	K3F10	K3C16		K3C20
	nozzle 0.5 (5)	K5F10		K5F20	

3. STATISTICAL ANALYSIS OF THE SPRAY IMAGES

The analysis of images generally starts from the definition of a region of interest, to be separated from the residual part of image, referred to as background. In the case of a sprayed jet, the zone on which one would focus attention is the portion of the image where liquid fragments intercept a line of sight between the illuminating source and the image-capturing device. The interposition of drops causes a local attenuation of the intensity of the collected light signal, essentially due to absorption and scattering phenomena. Operatively the separation between the spray region and the background is performed by assigning a threshold value to the light signal extinction, and thus cutting off all the parts of the image for which the light attenuation is weaker than the level fixed by the threshold value. The choice of the threshold value would be somewhat easier if the distribution of light extinction intensity were bimodal. Unfortunately in the case studied in this paper the progressive liquid atomization and droplet dispersion result in the presence of slight gradients over the image, preventing a straightforward individuation of a criterion of separation between spray and background. As matter of fact a peculiarity of the images of liquid jets in crossflow is the existence of steep gradients on the windward side of the spray and of much more progressive gradients on the leeward side. As a consequence the choice of the threshold value has little effect on the appearance of the windward spray profile, and then it did not represent a critical point for the reconstruction of the jet trajectory [12]. Aiming to evaluate the morphological and dynamical aspects of the whole spray plume, the chance to achieve a "correct" choice of the threshold level is at the same time relevant and somehow arbitrary. Missing indeed a step transition from the spray to the background, the selection of a cut-off value has to match the requirement of how much of the spray one wants to focus on. In the image analysis presented in this paper it was decided to set a threshold value equal to the 50% of the maximum value of light extinction detected over a whole set of images, and so a different value was assigned to each set, in order to sweep off any accidental variation in the illumination conditions.

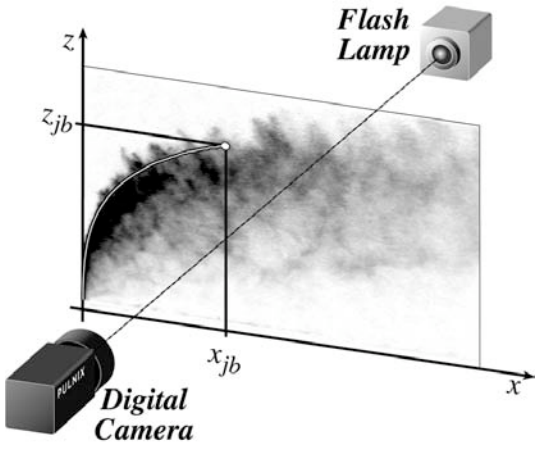

Fig. 1. Sketch of the diagnostic setup and coordinate system.

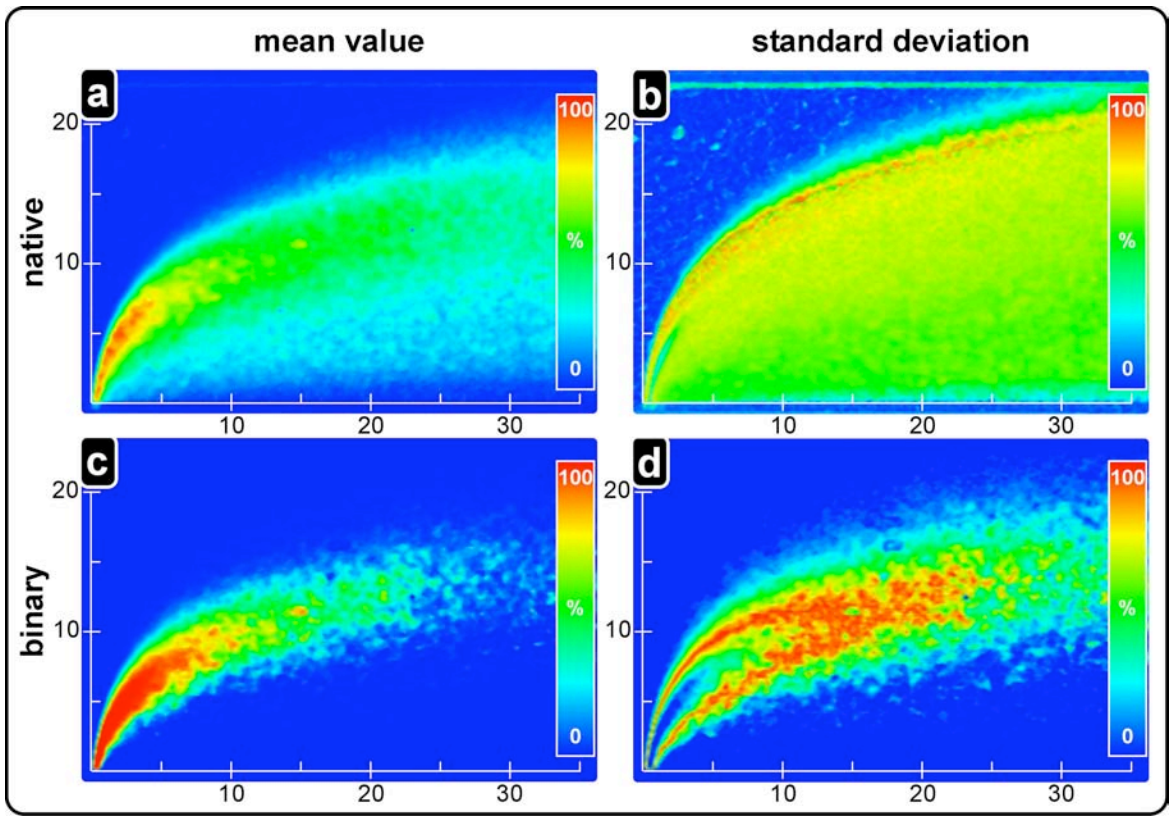

Fig. 2. Four images representing, pixel by pixel, the mean and the standard deviation of light extinction intensity (native images) and spray occurrence (binary images) . Distances are in mm. (Test case: W5F20, V_L = 23 m/s, V_G = 26 m/s)

Beside the problem of discriminating between spray and background, another critical point is the unsteadiness of the spray plume. This means that in a set of N images, captured in sequence by keeping unchanged the operating conditions, some general aspects of the spray are common to the N events, being they different from each other. A statistical approach is interested in evaluating both the common features, which define the average behavior of the spray, and the elements that differentiate each individual occurrence of the spray from the average. In other words, chosen a non-deterministic property detectable from each image of a statistic sample, object of this study is the mean value and the standard deviation of the property over the sample.

The simplest property to be evaluated over a set of digital images is whether the spray "occupies" a certain pixel or not. This can be easily obtained by replacing the extinction signal of a pixel by a "1" if the value in that pixel overcomes the threshold value, and by a "0" if it does not. This simple non-linear operation allows creating a "binary" image starting from a "native" image; the inverse operation is obviously unfeasible.

Fig. 2 reports four different images that can be generated by evaluating, pixel by pixel, the mean and the standard deviation of light extinction intensity (native images) and occurrence (binary images) of the spray. The intensity scale is normalized to the maximum. The reference case for this and all the following images is water injected at 23 m/s from a 0.5 mm plain nozzle in 20 bars and 600 K air crossflow at 26 m/s.

4. THE CENTERLINE OF THE SPRAY

The average native image (Fig. 2a) appears quite different from the average binary image (Fig. 2c), being the latter characterized by the fact that each pixel embeds a value, in the range between 0 and N, which represents the probability that the spray intercepts the line-of-sight individuated by that pixel. The image is characterized by the zero-probability of the whole background, whereas in the spray zone the probability grows as one moves from the boundary to the centerline of the spray (see Fig. 3). In other words it can be stated that, supposing to move along a curvilinear coordinate following the spray stream, the plane normal to each point of the coordinate identifies a probability distribution, as showed in Fig. 4. Given such a curvilinear coordinate, the whole average binary image can be reconstructed as a succession of probability profiles, and each of them can be replaced by a normal distribution. In Fig. 5 an example of some of the normal distributions is plotted. The successfulness of such interpolation is mainly connected to the symmetry of the distribution. The choice of a cut-off threshold of 50% is actually meant to discard enough of the leeward spray plume, so that a good level of symmetry is achieved. The locus of the medians of all the interpolating normal distributions laying along the curvilinear coordinate is defined as the *centerline* of the spray, and it is indeed the curvilinear coordinate that represents the spray stream. In Fig. 5 the centerline can be made up as the projection of the blue points on the xz plane.

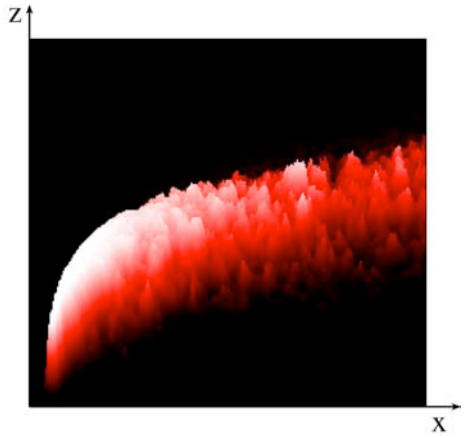

Fig. 3. Average binary image in 3D view.

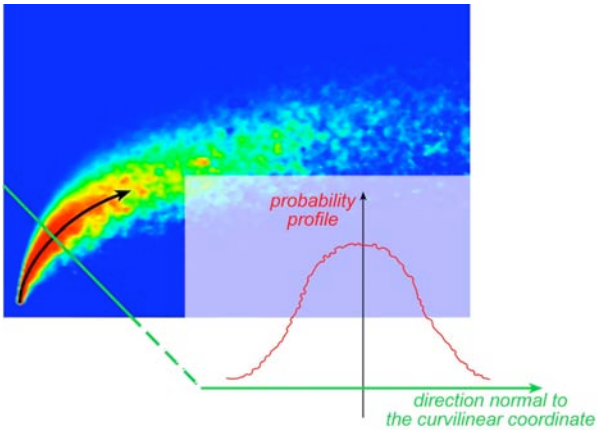

Fig. 4. Example of probability profile at a value of curvilinear coordinate.

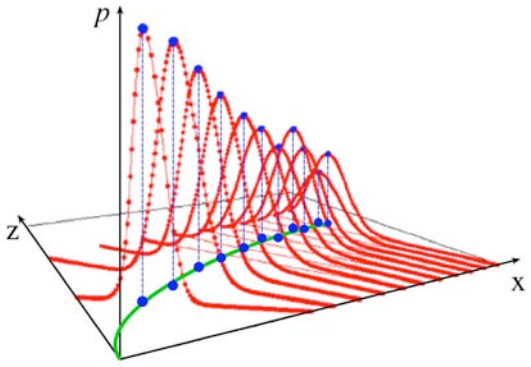

Fig. 5. Normal distributions replacing the probability profiles for a reduced number of centerline points.

It is obvious that the operative determination of the centerline requires that the same centerline is known, and so an iterative procedure has to be set up. As first-step estimation of the centerline is chosen the liquid jet trajectory, defined and experimentally determined in [12] as the average of the windward boundary of the sampled binary images. It must be stressed that the above-explained procedure for the evaluation of the maxima of the normal distributions is actually little sensitive to the tentative value. As a consequence, the iterative calculation rapidly converges to the correct solution. As matter of fact it has been verified that the third-step resulting centerline does not significantly differ from the second step.

5. INSTABILITY AND INTERMITTENCY OF THE SPRAY

The variance of the native image (Fig. 2c) can be seen as a plot of the instability field of the spray, being the value associated to each pixel representative of the level of local unsteadiness of the light signal attenuation due to the interposition of liquid fragments and drops. This image typically shows a rather uniform instability throughout the wall region covered by the spray, with a little and gradual increase of the light attenuation flickering as one moves towards the upper edge of the spray. This behavior is probably due to the presence, near to the wall housing the injector, of a fine spray (stripped from the liquid jet by the airflow), whose granulometry and spatial distribution result in a low level of fluctuation of the detected light signal. By rising up to the top edge of the spray, the presence of larger fragments, still to be further atomized, is supposed to be responsible of a worse dispersion in the gas phase, as testified by the slightly higher flickering of the signal.

Differently, the variance of the binary image (Fig. 2d) depicts the intermittency field of the spray. This parameter does not consider the stochastic flickering due to the local, even small, fluctuations of the light extinction signal. The intermittency is a measure of the *overall* unsteadiness of the spray cloud, probably attributable to the whipping of the liquid jet. The pixels with higher values are characterized by a higher uncertainty to find there the spray, and typically the maximum uncertainty is localized in the surroundings of the spray boundary.

Incidentally, it must be noted that Figs. 2c and 2d are not independent from each other. As matter of fact, due to the circumstance that each pixel can assume value either 0 or 1, the mean value μ (probability) and the standard deviation σ (uncertainty) are correlated as:

$$\sigma = \sqrt{\mu(1-\mu)} \tag{4}$$

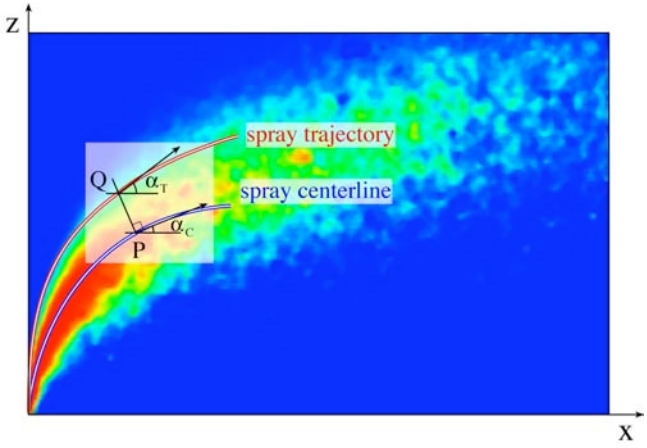

Fig. 6. Definition of the spray angle.

6. ANGLE OF SPRAY

The concept of angle of spray was introduced in the framework of liquid injected in quiescent or co-flowing air. It is meant as a measure of the dispersion of the liquid in the gas phase. In the case of liquid injected in crossflowing airstream, the bending of the spray due to the airflow makes it hard to define a parameter analogous to the spray angle. The definition proposed in this paper is based on the above-introduced concept of centerline. By assuming the centerline as corresponding to the injection axis of a jet in still air, the profile of the distance of the jet trajectory from the centerline is calculated and the average value of the slope of this profile is defined as spray angle. Obviously the same result is achieved by evaluating, for each point P of the centerline, the average difference between the angle α_C of the centerline, with respect to the x-axis parallel to the airflow, and the angle α_T of the jet trajectory at the point Q intercepted by the normal to the centerline in P (see Fig. 6).

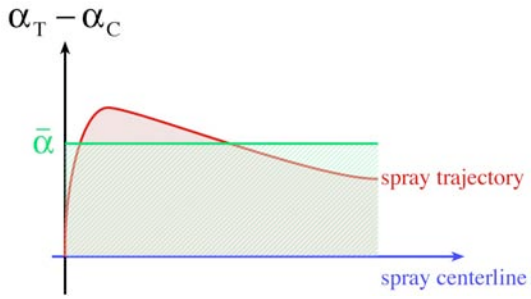

Fig. 7. Typical profile of the spray angle along the curvilinear coordinate.

The spray trajectory can be well described by a power law curve, as already pointed out in [12]. Analogously it has been seen that also the spray centerline can be replaced by a curve $z = k \cdot x^{\beta}$, being the parameters k and β evaluated by best-fit criterion. The availability of analytical expressions for trajectory and centerline simplifies the spray angle calculation.

The behavior depicted by the red line in Fig. 7 appeared to by common to all cases. Actually both the mean and the maximum value of the spray angle were evaluated. As regards the maximum of the red curve, it resulted to be quite sensitive to the experimental noise, while the data obtained for the average spray angles are presented in Fig. 8, plotted against the liquid Weber number, defined as $We_L = \rho_L V_L^2 D/\sigma$, which in the performed experiments was varied between about 10^3 and 10^5. The values of spray angle range roughly from 5° and 50°. Although the points are quite scattered, the average spray angle shows an unmistakable trend to grow up as We_L increases. This seems to indicate that the achievement of a good level of dispersion of the liquid, at least as concerns the z axis, mainly depends on the capacity to provide enough kinetic energy to the liquid, whereas the gas kinetic energy should be suitable to assure correct placing of the dispersed phase within the premixing duct.

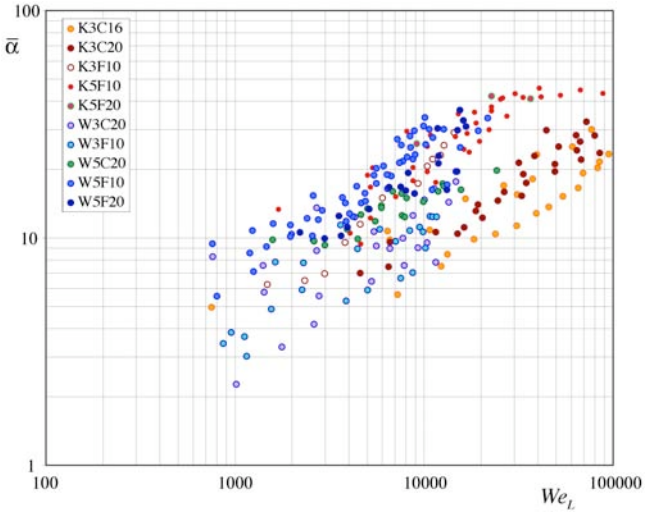

Fig. 8. Dependence of the spray angle, in degrees, on We_L.

Both the wide dispersion of points on the plot and the behavior of the single groups of data plotted in Fig. 8 induced to hypothesize that the spray angle also depends on other parameters. An attempt to infer a multiple correlation is not easy, due to the data scattering indeed, anyway it has been observed that the data well scale with the orifice diameter. As a consequence the liquid Weber number and the orifice diameter (divided by a reference value $D_0 = 0.5$ mm to keep it dimensionless) have been chosen as independent variables to perform a non-linear regression of the spray angle data. The resulting best fitting correlation is:

$$\bar{\alpha} = 0.538 \left(\frac{D}{D_0} \right)^{1.358} We_L^{0.405} \qquad (5)$$

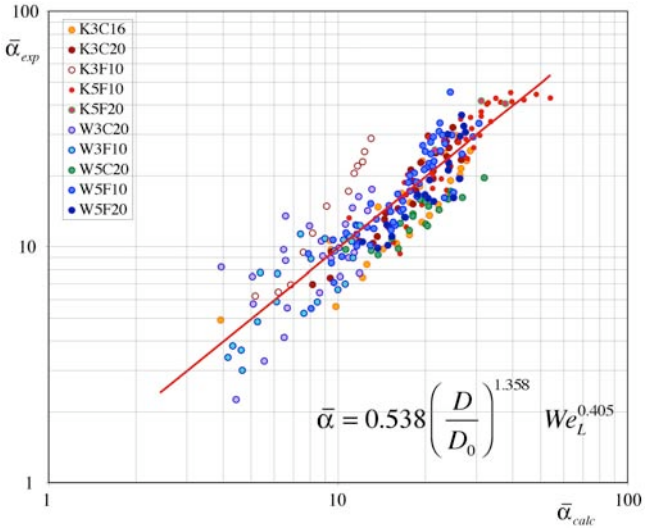

Fig. 9. Dependence of the spray angle on liquid Weber number and dimensionless orifice diameter.

Fig. 9 compares experimental (in ordinate) and calculated values (in abscissa) of the spray angle. The closer the points are to the red bisecting line, the better is the prediction. The correlation coefficient for Eq. (5) was assessed as 0.861. Equation (5) does not provide any effect of the gas kinetic energy on the spray angle. This hypothesis was tested by introducing a third independent variable, the gas Weber number $We_G = \rho_G V_G^2 D/\sigma$. The dependence on We_L and the orifice diameter being kept frozen, a further non-linear regression was performed and the resulting best fitting correlation

$$\bar{\alpha} = 1.05 \left(\frac{D}{D_0} \right)^{1.358} We_L^{0.405} \; We_G^{-0.123} \qquad (6)$$

showed an improvement in the prediction ability, since the correlation coefficient rose to 0.882. Anyway the effect of gas Weber number appears to be less relevant than We_L and injection diameter, and this consideration holds even if the non-linear regression is performed on the three parameters simultaneously:

$$\bar{\alpha} = 0.433 \left(\frac{D}{D_0} \right)^{1.358} We_L^{0.588} \; We_G^{-0.289} \qquad (7)$$

In this last case a little increase of the We_G exponent was observed, indicating that Eq. (6) probably underestimated the effect of gas momentum. On the other hand the parallel increase of the exponent of liquid Weber number indicates that Eq. (6) well predicts the dependence on the capillary pressure σ/D, being in both Eqs. (6) and (7) expressed by an exponent of about 0.3. The modification of the orifice diameter dependence was very little, and so the exponent in Eq. (7) was kept the same as Eq. (6). Equation (7) resulted to be the best of the proposed correlations, with correlation coefficient equal to 0.901. The corresponding plot is reported in Fig. 10.

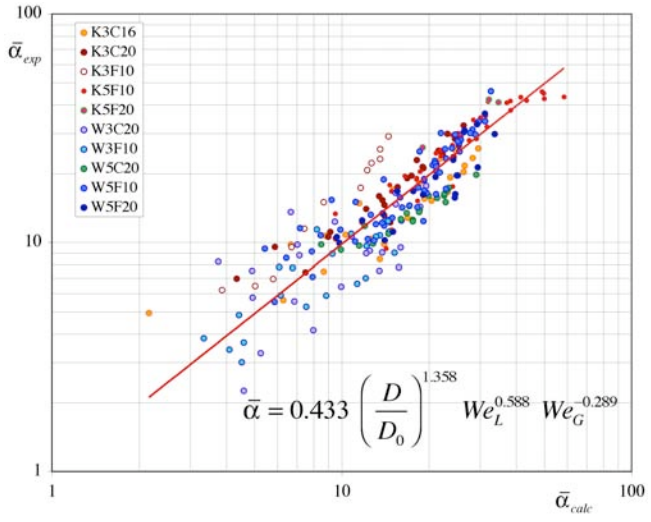

Fig. 10. Dependence of the spray angle on both liquid and gas Weber number and dimensionless orifice diameter.

7. NORMALIZED INTERMITTENCY INDEX

The above-presented Figs. 2b and 2d plot the standard deviation of native and binary images, respectively. It can be observed that in both images there is a region, near the injection point, characterized by values noticeably lower than the surrounding pixels. This fact can be quite plainly understood in the case of binary images, since it is expectable that a number of pixels have value constantly equal to 1 for all the 1000 sampled images, thus for those pixels the standard deviation is zero. Differently for the native image (Fig. 2b) there is a smaller group of pixels, whose values of light extinction intensity have low but non-zero variance. The region so individuated has not only no intermittency, which is reasonable since the proximity to the injection point prevents significant whipping, but it is also extremely stable, which seems to indicate that the attenuation of the light signal is attributable not only to the interposition of traveling droplets and fragments, but mainly to the presence of a more stable object, supposedly the liquid jet itself. The presence of this "virtual" liquid core was systematically observed for all test conditions, but a quantitative characterization has not been performed yet.

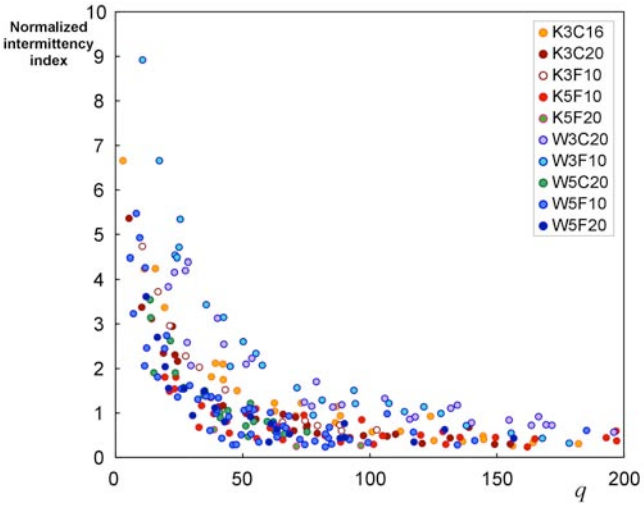

Fig. 11. Normalized intermittency index as a function of liquid-to-air momentum ratio q.

The standard deviation of the binary images can be further exploited to define a synthetic parameter accounting for the overall level of intermittency of the spray. This parameter is obtained simply by summing the intermittency over all the pixels of the image in Fig. 2d. The availability of such parameter allows investigating the possible dependence of spray intermittency on the operating conditions. Aiming to avoid the biasing effect of the amount of injected liquid on the calculated value, the intermittency index was normalized by the average area of the sampled binary images. The resulting index was successfully plotted as a function of the liquid-to-air momentum ratio q,

$$q = \frac{\rho_L V_L^2}{\rho_G V_G^2} \qquad (5)$$

as reported in Fig. 11. The intermittency of the spray is high for low q values, therefore rapidly drops as q increases, and above $q \approx 50$ is nearly constant. It was observed that the spread of the data points could be reduced by introducing a further dependence on the dimensionless orifice diameter. Quite surprisingly, the exponent to be assigned to the dimensionless diameter to best reduce the data spread is very close to the value found before for the spray angle, as results in Fig. 12. The last figure also points out that kerosene points (in orange) place slightly below the water points (in blue). It is possible to suppose that the larger tendency to atomize of kerosene is responsible of a little lower level of whipping, although this effect has never been observed before.

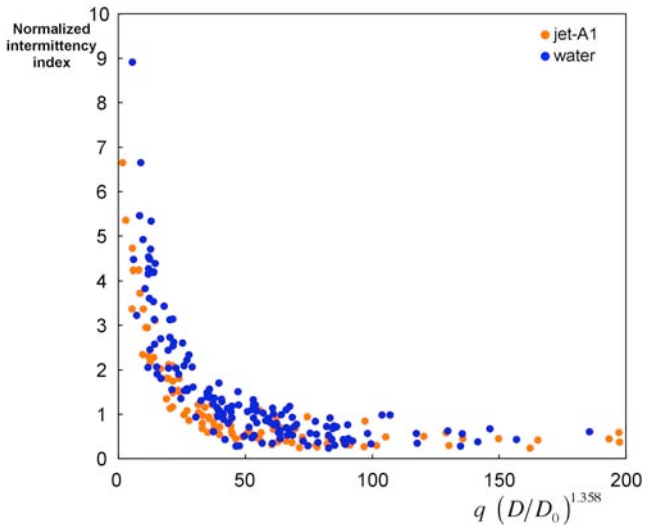

Fig. 12. Effect of the orifice diameter on the intermittency index. Data points are grouped only by test liquid.

8. CONCLUSIONS

A novel approach to the characterization of liquid jets in crossflow has been presented. Statistical analysis of large samples of spray images allowed for getting information about morphology and stability of the spray. From the analysis of the average binary image, representing a kind of probability map, the definition of spray centerline has been attained. This line can be seen as a curvilinear coordinate to investigate how spray properties evolve along the liquid mean stream. As an example of this, in this paper the evolution of the distance of the jet trajectory from the centerline has been used to introduce a definition of spray angle in the case of crossflow atomization. The study proved that the spray spread in the z direction is mainly connected to the value of liquid Weber number, as well as on the orifice diameter. The introduction of a weaker dependence on the gas Weber number did not affect the overall dependence on capillary pressure.

The concepts of instability and intermittency were discussed. The former is meant as a measure of the local unsteadiness of the light signal attenuation, due to the interposition of traveling liquid fragments. The study has showed the great stability of a small region, near the injection point, suggesting the existence of a stable liquid core. The intermittency is probably linked to the phenomenon of jet whipping. A normalized intermittency index was defined and showed to decrease with the liquid-to-air momentum ratio q and scale with the orifice diameter.

9. ACKNOWLEDGEMENTS

This work has been partly supported by the European Community in the framework of the MUSCLES contract, Growth project GRD1-2001-40198. Authors wish to thank Fabio Mancuso and Pietro Scoppetta for their valuable help in the experimental work.

10. REFERENCES

[1] Wu, P.K., Kirkendall, K.A., Fuller, R.P., Nejad, A.S., Breakup processes of liquid jets in subsonic crossflows, Journal of Propulsion and Power, Vol. 13, pp. 64–73, 1997.

[2] Becker, J. and Hassa, C., Breakup and Atomization of a Kerosene Jet in Crossflow at Elevated Pressure, Atomization and Sprays, Vol. 11, pp. 49-67, 2002.

[3] Rachner, M., Becker, J., Hassa, C., Doerr, T., Modelling of the Atomization of a Plain Liquid Fuel Jet in Crossflow at Gas Turbine Conditions, Aerospace Science and Technology, Vol. 6, pp. 495-506, 2002.

[4] Schetz, J.A., Kush, E.A. Jr., Joshi, P.B., Wave Phenomena in Liquid Jet Breakup in a Supersonic Crossflow, AIAA Journal, Vol. 18, pp. 774-778, 1979.

[5] Chen, T.H., Smith, C.R., Schommer, D.G., Nejad, A.S., Multi-Zone Behavior of Transverse Liquid Jet in High-Speed Flow, AIAA Paper 93-0453, 1993.

[6] Oda, T., Nishida, K., Hiroyasu, H., Charaterization of Liquid Jet Atomization across a High Speed Airstream by Laser Sheet Tomography, Proc. 6th International Conference on Liquid Atomization and Spray Systems (ICLASS '94), pp. 624-631, 1994.

[7] Ragucci, R. and Cavaliere, A., Identification of Cross-flow Liquid-jet Structures by means of Statistical Image Evaluation, Proc. 18th Annual Conference on Liquid Atomization and Spray Systems (ILASS-Europe '02), paper 89, 2002.

[8] Ragucci, R., Bellofiore, A., Carulli, G., Cavaliere, A., Momentum Coherence Breakdown of Bending Atomizing Liquid Jet, Proc. 9th International Conference on Liquid Atomization and Spray Systems (ICLASS '03), paper 1-13, 2003.

[9] Cavaliere, A., Ragucci, R., Noviello, C., Bending and Break-up of a Liquid Jet in a High Pressure Airflow, Experimental Thermal and Fluid Science, Vol. 27, pp. 449-454, 2003.

[10] Ragucci, R., Bellofiore, A., Cavaliere, A., Statistical Evaluation of Dynamics and Coherence Breakdown of Kerosene and Water Jets in Crossflow, Proc. 19th Annual Conference on Liquid Atomization and Spray Systems (ILASS-Europe '04), pp. 44-49, 2004.

[11] Bellofiore, A., Di Martino, P., Ragucci, R., Cavaliere,

A., Experimental and Numerical Investigation on a Liquid Jet Injected in a High Pressure Channel, Proc. 20th Annual Conference on Liquid Atomization and Spray Systems (ILASS-Europe '05), pp. 451-456, 2005.

[12] Ragucci, R., Bellofiore, A., Cavaliere, A., Trajectory and Momentum Coherence Breakdown of a Liquid Jet in High-Density Air Crossflow, Atomization and Sprays 2006 (in press).

[13] Ragucci, R., Bellofiore, A., Cavaliere, A., Breakup and Breakdown of Bent Kerosene Jets in Gas Turbine Conditions, Proc. 31st International Symposium on Combustion, 2006 (in press).

[14] Nejad, A.S. and Schetz, J.A., Effects of viscosity and surface tension on a jet plume in supersonic flow, AIAA Journal, Vol. 22, pp. 458-459, 1983.